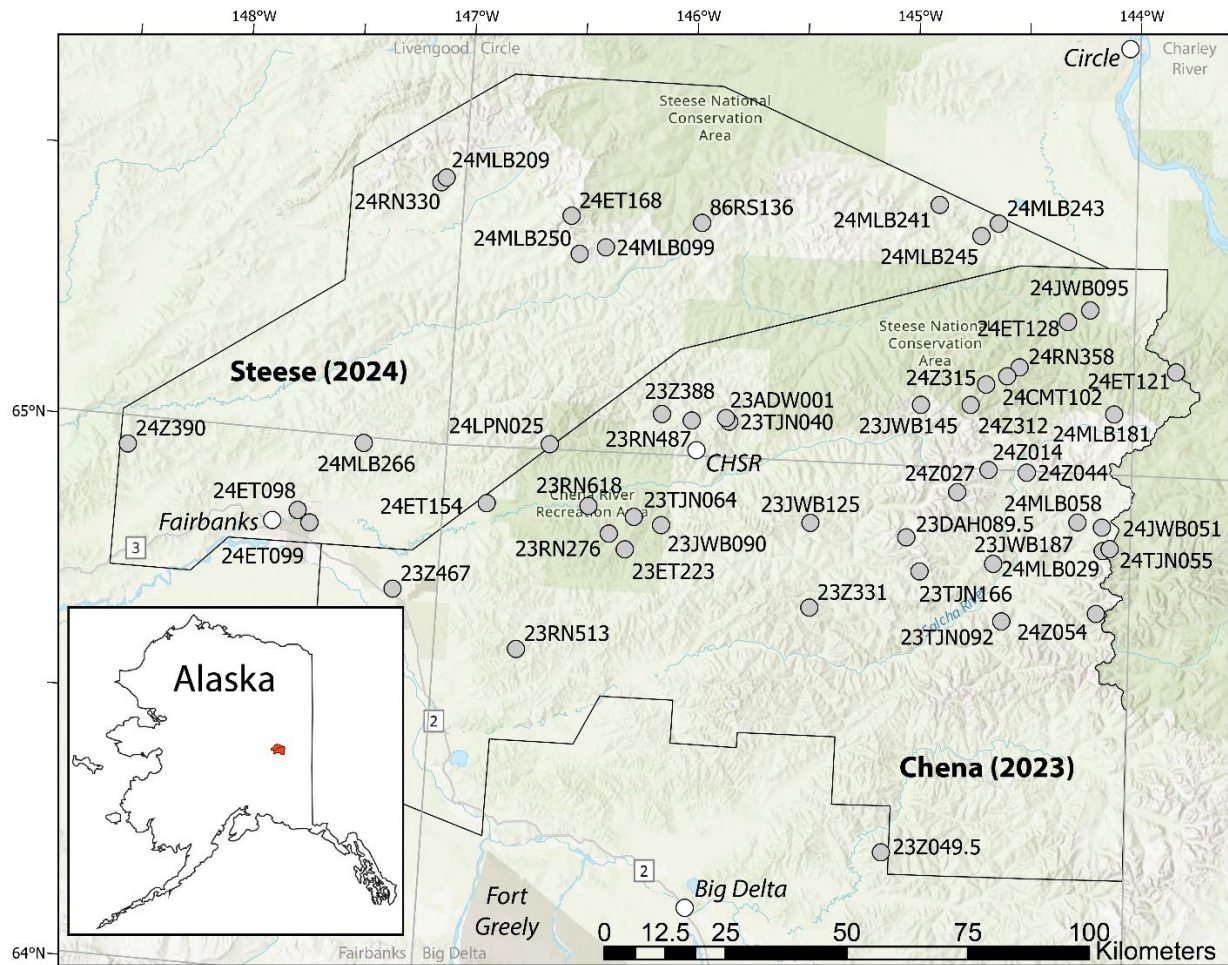


# LA-ICP-MS URANIUM-LEAD ZIRCON DATA FROM SAMPLES IN THE CHENA AND STEESE PROJECT AREAS

J. Wesley Buchanan, Michael L. Barrera, Jamshid A. Moshrefzadeh, Conner M. Truskowski, and Rainer J. Newberry

## Raw Data File 2025-25



Location map of samples selected for uranium-lead geochronologic analysis. The polygons outlined in black represent Earth MRI project areas and are labeled with the project name and year of award funding. CHSR is the location of Chena Hot Springs Resort. Light gray lines and text show the 1:250,000 quadrangle boundaries and name.

This report has not been reviewed for technical content or for conformity to the editorial standards of DGGS.

2025

STATE OF ALASKA

DEPARTMENT OF NATURAL RESOURCES

DIVISION OF GEOLOGICAL & GEOPHYSICAL SURVEYS



## STATE OF ALASKA

Mike Dunleavy, Governor

## DEPARTMENT OF NATURAL RESOURCES

John Crowther, Commissioner

## DIVISION OF GEOLOGICAL & GEOPHYSICAL SURVEYS

Erin A. Campbell, State Geologist & Director

Publications produced by the Division of Geological & Geophysical Surveys are available to download from the DGGs website ([dgggs.alaska.gov](https://dgggs.alaska.gov)). Publications on hard-copy or digital media can be examined or purchased in the Fairbanks office:

### Alaska Division of Geological & Geophysical Surveys (DGGs)

3354 College Road | Fairbanks, Alaska 99709-3707

Phone: 907.451.5010 | Fax 907.451.5050

[dggspubs@alaska.gov](mailto:dggspubs@alaska.gov) | [dgggs.alaska.gov](https://dgggs.alaska.gov)

### DGGs publications are also available at:

Alaska State Library, Historical  
Collections & Talking Book Center  
395 Whittier Street  
Juneau, Alaska 99801

Alaska Resource Library and  
Information Services (ARLIS)  
3150 C Street, Suite 100  
Anchorage, Alaska 99503

### Suggested citation:

Buchanan, J.W., Barrera, M.L., Moshrefzadeh, J.A., Truskowski, C.M., and Newberry, R.J., 2025, LA-ICP-MS uranium-lead zircon data from samples in the Chena and Steese project areas.: Alaska Division of Geological & Geophysical Surveys Raw Data File 2025-25, 4 p. <https://doi.org/10.14509/31731>



# LA-ICP-MS URANIUM-LEAD ZIRCON DATA FROM SAMPLES IN THE CHENA AND STEESE PROJECT AREAS

J. Wesley Buchanan<sup>1</sup>, Michael L. Barrera<sup>1</sup>, Jamshid A. Moshrefzadeh<sup>1</sup>, Conner M. Truskowski<sup>1</sup>, and Rainer J. Newberry<sup>1</sup>

## INTRODUCTION

This dataset contains uranium-lead (U-Pb) geochronologic data and trace and rare earth element (TREE) data from single zircon spots analyzed using laser ablation inductively coupled plasma mass spectrometry (LA-ICP-MS). The two methods were run concurrently resulting in U-Pb age data and TREE data from the same zircon volume. Alaska Division of Geological & Geophysical Surveys (DGGs) staff collected zircon data from 51 samples of igneous and meta-igneous rocks primarily collected during the 2024 field season in support of the Earth Mapping Resources Initiative (Earth MRI) Steese and Chena projects. The goal of this dataset is to delineate the age of igneous activity to support geologic mapping efforts, tectonic interpretations, and characterization of mineralization in the Yukon-Tanana Uplands, Alaska.

Data are organized in the age summary data table with our interpreted crystallization ages, sample location information, and sample descriptions. The zircon grain data table contains U-Pb isotopic age data and TREE data for each zircon spot analyzed. Both tables have accompanying data dictionaries. Data are available on the DGGs website at <https://doi.org/10.14509/31731>.

## METHODS

This report includes single-grain zircon data generated by DGGs geologists at the Arizona LaserChron Center (ALC) at the University of Arizona with direction from laboratory staff. Whole-rock samples were sent to the ALC where they were cleaned and processed through a jaw crusher and roller mill. Zircon grains were isolated using magnetic separation and gravimetric separation with methylene iodide (MI). “Soft” minerals, those that are highly damaged, fractured, altered, or are otherwise less resistant, were removed using a Wig-L-Bug amalgamator, if necessary. Pyrite and apatite were removed by acid wash before hand-picking of zircon grains, if necessary. Approximately 60 zircon grains were selected from each isolated mineral separate to mount in 1-inch-diameter epoxy pucks. Back-scatter electron (BSE), cathodoluminescence (CL), and transmitted light images were collected. Some zircon grains were analyzed in multiple areas to investigate complex internal textural variations (e.g., convoluted zoning, inherited cores, etc.) revealed by CL and (or) BSE imaging.

LA-ICP-MS data were collected with an Element2 HR mass spectrometer. Zircon were targeted and ablated with a Teledyne/Photon Machines Analyte G2 excimer laser equipped with HelEx. Roughly forty, 30- $\mu$ m-diameter zircon spots were analyzed for most samples. Sample 24ET098 had more zircon grains mounted and analyzed because

---

<sup>1</sup>Alaska Division of Geological & Geophysical Surveys, 3354 College Road, Fairbanks, AK 99709

the sample was a meta-rhyolite tuff from the greenschist-grade Butte Formation. This sample was expected to have grains with lead loss or other isotopic disturbances as seen in other previous Butte samples. Gabbro sample 23JWB125 had more grains mounted because mineral separation yielded few zircon grains and all recovered zircon were mounted and imaged. Due to the expected older age of the sample, the likelihood of isotopic disturbance was higher. Data from zircon grains with disturbed isotopic systems cannot be included in crystallization age calculations; therefore, more grains were dated from both samples to increase the likelihood of gathering enough zircon analyses for a statistically robust age.

Before the collection of isotopic data, spots were cleaned using rapid-burst laser shots with 50- $\mu\text{m}$ -diameter spot sizes to remove surface contamination. The ablated material was passed through helium to the plasma source. Isotopes measured for U-Th-Pb geochronology include:  $^{204}\text{Pb}$ ,  $^{206}\text{Pb}$ ,  $^{207}\text{Pb}$ ,  $^{208}\text{Pb}$ ,  $^{232}\text{Th}$ ,  $^{235}\text{U}$ , and  $^{238}\text{U}$ . Isotopes measured for TREE analysis include:  $^{27}\text{Al}$ ,  $^{29}\text{Si}$ ,  $^{31}\text{P}$ ,  $^{45}\text{Sc}$ ,  $^{49}\text{Ti}$ ,  $^{89}\text{Y}$ ,  $^{93}\text{Nb}$ ,  $^{139}\text{La}$ ,  $^{140}\text{Ce}$ ,  $^{141}\text{Pr}$ ,  $^{146}\text{Nd}$ ,  $^{152}\text{Sm}$ ,  $^{153}\text{Eu}$ ,  $^{157}\text{Gd}$ ,  $^{159}\text{Tb}$ ,  $^{164}\text{Dy}$ ,  $^{165}\text{Ho}$ ,  $^{166}\text{Er}$ ,  $^{169}\text{Tm}$ ,  $^{174}\text{Yb}$ ,  $^{175}\text{Lu}$ ,  $^{177}\text{Hf}$ ,  $^{181}\text{Ta}$ ,  $^{202}\text{Hg}$ ,  $^{204}(\text{Hg}+\text{Pb})$ ,  $^{206}\text{Pb}$ ,  $^{207}\text{Pb}$ ,  $^{208}\text{Pb}$ ,  $^{232}\text{Th}$ , and  $^{235}\text{U}$ . All TREE data is reported in parts per million (ppm). Standards FC-1 (Paces and Miller, 1993), SL-2 (Gehrels and others, 2008), and R33 (Black and others, 2004) were analyzed between unknowns using standard sample bracketing to monitor instrument drift over the entire session by checking for shifts in age of reference material relative to their known values as defined by isotope dilution thermal ionization mass spectrometry (ID-TIMS).

All analysis procedures followed the techniques documented by Gehrels and others (2008), Gehrels and Pecha (2014), Pullen and others (2018), and Sundell and others (2021). Isotopic data were reduced at ALC using the MATLAB-based program AgeCalcML (Sundell and others, 2021). Raw data were corrected for common Pb by the methods of Stacey and Kramers (1975) and Mattinson (1987). Raw data had backgrounds removed and isobaric interference accounted for. Preliminary isotopic ratios for  $^{206}\text{Pb}/^{238}\text{U}$ ,  $^{206}\text{Pb}/^{207}\text{Pb}$ , and  $^{208}\text{Pb}/^{232}\text{Th}$  were compared to accepted values of reference materials to determine fractionation factors for each ratio. Internal uncertainties were propagated using the methods of Gehrels and others (2008) and Gehrels and Pecha (2014).

Samples 24ET098 and 23JWB125 did not have TREE analysis run, because those samples had significantly smaller zircon than other samples. The 30- $\mu\text{m}$ -diameter ablation spot size needed for TREE collection was larger than most zircon in each sample. When analyzing only for isotopes required for U-Pb age dating, the spot size is reduced to 15- $\mu\text{m}$ -diameter, which could be accommodated by most grains.

## CALCULATION OF CRYSTALLIZATION AGES

The crystallization age summary table contains weighted mean ages and accompanying statistics for 42 samples. Weighted mean ages and mean squared weighted deviations were calculated with IsoplotR version 6.5 using the methods

described by Vermeesch (2018). Mean ages were calculated using the  $^{206}\text{Pb}/^{238}\text{U}$  age and reported in millions of years with analytical errors at the two standard deviations level.

The zircon grain data table includes isotopic ratios, lab-calculated ages, and elemental data for all zircon spot analyses. The ALC staff will reject individual spot analyses based on variations in the intensity of the “signal” coming into the mass spectrometer, high common Pb, high discordance, reverse discordance, and incorrect isotopic offsets. The column `analysis_error` in the zircon grain data table lists the reason or reasons for the ALC staff rejecting the analysis. The summary table gives the number of analyses (n) used in each mean calculation and the total number (N\_total) of analyses that passed through the ALC’s quality control procedures. N\_total is the number of all grains analyzed minus the number of grain analyses rejected by the lab (analyses with a value in the `analysis_error` column). The weighted mean age represents the interpreted time of igneous crystallization. Older inherited grains were not included in the mean age. The zircon grain data table contains a column indicating whether the single zircon spot age was used in the weighted mean calculation.

Nine samples could not have crystallization ages calculated. These samples either had very low, or no zircon recovered, the U-Pb system was disturbed due to low-grade metamorphism or younger hydrothermal events, or most grains were inherited and not related to the crystallization of the igneous body. Notes on why a crystallization age could not be calculated for a given sample can be found in the crystallization age summary table.

## ACKNOWLEDGMENTS

The authors thank the University of Arizona LaserChron Center staff for their contributions to data collection, technical discussions, and other support. The analytical work was funded by the U.S. Geological Survey’s Earth Mapping Resources Initiative (Earth MRI) under cooperative agreement G24AC00323 and by the State of Alaska. The views and conclusions contained in this document are those of the authors and should not be interpreted as representing the opinions or policies of the U.S. Geological Survey. Mention of trade names or commercial products does not constitute their endorsement by the U.S. Geological Survey.

## REFERENCES

Black, L.P., Kamo, S.L., Allen, C.M., Davis, D.W., Aleinikoff, J.N., Valley, J.W., Mundil, Roland, Campbell, I.H., Korsch, R.J., Williams, I.S., and Foudoulis, Chris, 2004, Improved  $^{206}\text{Pb}/^{238}\text{U}$  microprobe geochronology by the monitoring of trace-element-related matrix effect; SHRIMP, ID-TIMS, ELA-ICP-MS and oxygen isotope documentation for a series of zircon standards: *Chemical Geology*, v. 205, no. 1–2, p. 15–140, <https://doi.org/10.1016/j.chemgeo.2004.01.003>

- Gehrels, G.E., Valencia, V.A., and Ruiz, Joaquin, 2008, Enhanced precision, accuracy, efficiency, and spatial resolution of U-Pb ages by laser ablation-multicollector-inductively coupled plasma-mass spectrometry: *Geochemistry Geophysics Geosystems*, v. 9, 13 p., <https://doi.org/10.1029/2007GC001805>
- Gehrels, G.E., and Pecha, M.E., 2014, Detrital zircon U-Pb geochronology and Hf isotope geochemistry of Paleozoic and Triassic passive margin strata of western North America: *Geosphere*, v. 10, no. 1, p. 49–65
- Mattinson, J.M., 1987, U–Pb ages of zircons: A basic examination of error propagation: *Chemical Geology*, v. 66, p. 151–162, [https://doi.org/10.1016/0168-9622\(87\)90037-6](https://doi.org/10.1016/0168-9622(87)90037-6)
- Paces, J.B., and Miller, J.D., 1993, Precise U-Pb ages of Duluth Complex and related mafic intrusions, northeastern Minnesota: Geochronological insights to physical, petrogenic, paleomagnetic, and tectonomagmatic processes associated with the 1.1 Ga Midcontinent Rift System: *Journal of Geophysical Research*, v. 98, no. B8, p. 13,997–14,013, <https://doi.org/10.1029/93JB01159>
- Pullen, Alex, Ibáñez-Mejía, Mauricio, Gehrels, G.E., Giesler, Dominique, and Pecha, M.E., 2018, Optimization of a laser ablation-single collector-inductively coupled plasma-mass spectrometer (Thermo Element 2) for accurate, precise, and efficient zircon U-Th-Pb geochronology: *Geochemistry Geophysics Geosystems*, v. 19, no. 10, p. 3,689–3,705, <https://doi.org/10.1029/2018GC007889>
- Stacey, J.S., and Kramers, J.D., 1975, Approximation of terrestrial lead isotope evolution by a two-stage model: *Earth and Planetary Science Letters*, v. 26, p. 207–221
- Sundell, K.E., Gehrels, G.E., and Pecha, M.E., 2021, Rapid U-Pb geochronology by laser ablation multi-collector ICP-MS: *Geostandards and Geoanalytical Research*, v. 45, no. 1, p. 37–57, <https://doi.org/10.1111/ggr.12355>
- Vermeesch, Pieter, 2018, IsoplotR: A free and open toolbox for geochronology: *Geoscience Frontiers*, v. 9, p. 1,479–1,493, <https://doi.org/10.1016/j.gsf.2018.04.001>